

# Differentiation of Discordant Lesions on Dual-Tracer PET/CT ( $^{68}\text{Ga}$ -PSMA-11 and $^{18}\text{F}$ -FDG) in Prostate Carcinoma: Diagnosis of Second Primary Malignancies

Ashwini Chalikandy<sup>1,2</sup>, Subhash Yadav<sup>2,3</sup>, and Sandip Basu<sup>1,2</sup>

<sup>1</sup>Radiation Medicine Centre, Bhabha Atomic Research Centre, Tata Memorial Hospital Annexe, Mumbai, India; <sup>2</sup>Homi Bhabha National Institute, Mumbai, India; and <sup>3</sup>Department of Pathology, Tata Memorial Hospital, Mumbai, India

We present 2 cases of metastatic castration-resistant prostate carcinoma with discordant lesions on dual-tracer PET/CT ( $^{68}\text{Ga}$ -PSMA-11 and  $^{18}\text{F}$ -FDG PET/CT), which on subsequent histopathologic evaluation revealed second primary malignancies of combined hepatocellular carcinoma and cholangiocarcinoma and poorly differentiated squamous cell carcinoma. These case illustrations emphasize the need to evaluate discordant lesions on dual-tracer PET/CT, which can lead to early diagnosis of second primary malignancies and thereby can provide better management in these patients.

**Key Words:** prostate carcinoma; dual-tracer PET/CT;  $^{68}\text{Ga}$ -PSMA-11;  $^{18}\text{F}$ -FDG; second primary malignancy

J Nucl Med Technol 2023; 00:1–4  
DOI: 10.2967/jnmt.123.265779

Prostate cancer is the most commonly diagnosed malignancy in men worldwide and the fifth leading cause of cancer-related death in men (1). The major risk factors for prostate cancer are age, Black ethnicity, obesity, and family history (2). Second primary malignancies (SPMs) are either synchronous or present as serious long-term complications in cancer survivors and necessitate early diagnosis and management. Various hypotheses have been put forward to explain the occurrence of SPMs in patients with carcinoma of the prostate. First, the SPMs can be due to detection bias, as the patients undergo multiple diagnostic

procedures after the detection of primary prostate cancer. Some literature data show that there may be an increased risk of SPMs in prostate cancer patients after treatment such as androgen deprivation therapy (3) and radiotherapy (4–7). In patients with metastatic castration-resistant prostate carci-

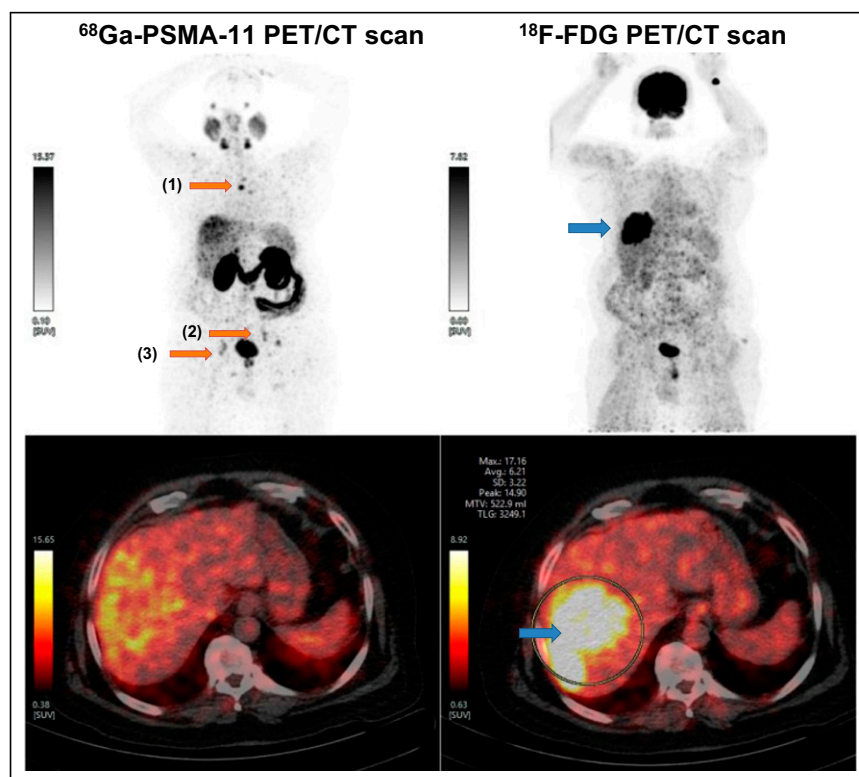


**FIGURE 1.** Whole-body  $^{68}\text{Ga}$ -PSMA-11 PET/CT and  $^{18}\text{F}$ -FDG PET/CT scans showing  $^{68}\text{Ga}$ -PSMA-11 expression (orange arrows) in sclerotic skeletal lesions in body of D4 vertebra (lesion 1), in left internal iliac lymph nodes (lesion 2), and bilaterally in pelvic bones (lesion 3); none of these showed any  $^{18}\text{F}$ -FDG uptake. Hypodense lesion in segment VII/VIII of liver showed  $^{18}\text{F}$ -FDG uptake (blue arrow) but did not show any significant  $^{68}\text{Ga}$ -PSMA-11 expression, raising suspicion and requirement of further confirmation.

Received Apr. 21, 2023; revision accepted Jul. 6, 2023.  
For correspondence or reprints, contact Sandip Basu (drsamb@yahoo.com).  
Published online Aug. 16, 2023.  
COPYRIGHT © 2023 by the Society of Nuclear Medicine and Molecular Imaging.

noma,  $^{68}\text{Ga}$ -PSMA-11 and  $^{18}\text{F}$ -FDG PET/CT scans provide complementary information and have been used to assess eligibility for prostate-specific membrane antigen (PSMA)-targeted radioligand therapy. The quantitative parameters of

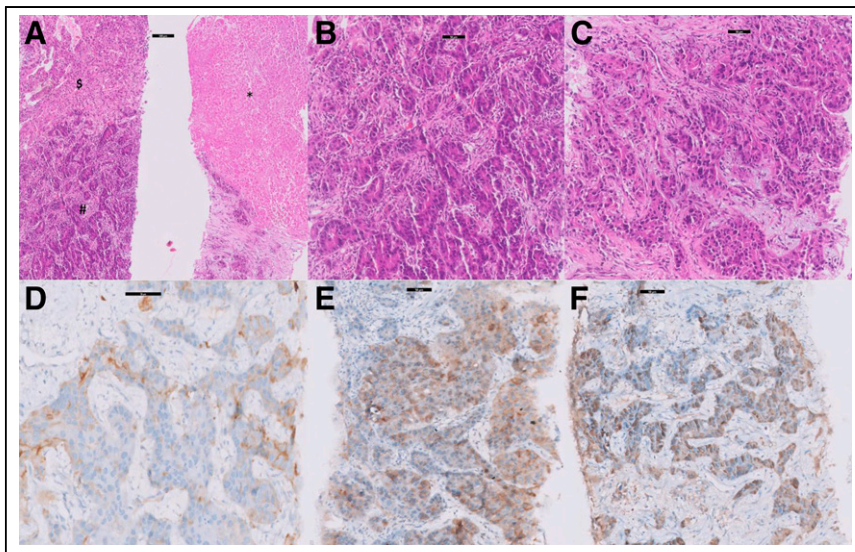


**FIGURE 2.** (A) Scanner view showing tumor with dual morphology. Lower half of left image shows tumor arranged in glandular architecture resembling adenocarcinoma (#), whereas upper half shows tumor arranged in broad trabeculae resembling hepatocellular carcinoma (\$). On right, biopsy core shows necrosis (\*) (hematoxylin and eosin,  $\times 40$ ). (B) Tumor arranged in glandular architecture, with large cells having moderate nuclear atypia resembling adenocarcinoma (hematoxylin and eosin,  $\times 100$ ). (C) Tumor cells arranged in large nodules and thickened trabeculae with moderate nuclear atypia and eosinophilic cytoplasm suggesting hepatocytic neoplasm (hematoxylin and eosin,  $\times 100$ ). (D) Glandular tumor (adenocarcinoma) component positive for CK7 (immunohistochemistry,  $\times 100$ ). (E and F) Hepatocytic tumor (hepatocellular carcinoma) component positive for glypican-3 (E) and arginase (F) (immunohistochemistry,  $\times 100$ ). Scale bars denote 50  $\mu\text{m}$ .

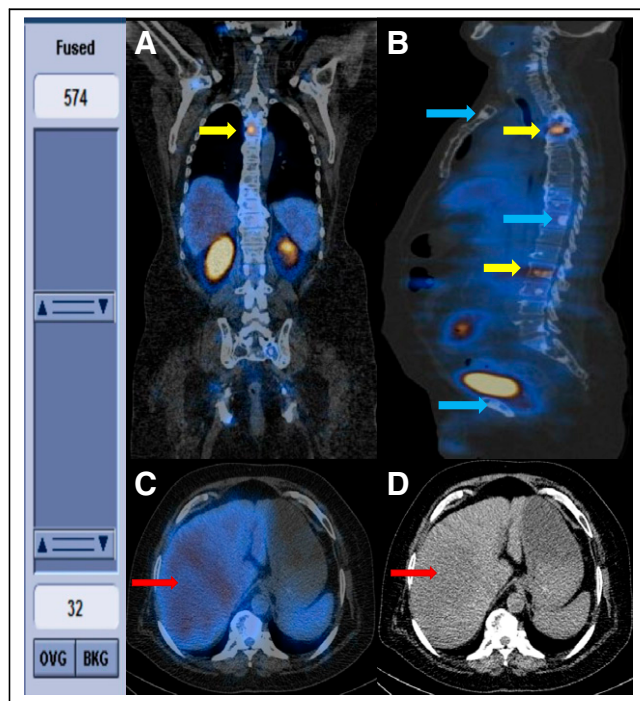


**FIGURE 3.** Coronal (A) and axial (B) posttherapy SPECT/CT images showing  $^{177}\text{Lu}$ -PSMA-617-expressing (yellow arrows) and nonexpressing (blue arrows) multiple sclerotic skeletal lesions. Transaxial SPECT/CT (C) and CT (D) posttherapy images showing hypodense lesion in segment VII/VIII of liver (arrow), with absence of  $^{177}\text{Lu}$ -PSMA expression.

these scans have potential to be used as a tool for treatment selection, disease prognostication, and evaluation of the response to administered therapy (8–10). Here, we report 2 cases of metastatic castration-resistant prostate carcinoma with discordant lesions on dual-tracer PET/CT, finally turning out to be metachronous secondary primary malignancies on biopsy.

#### Case 1

A 62-y-old man presented with persistent fever and severe backache. MRI of the dorsolumbar spine showed multiple focal lesions with altered signal intensity in visualized vertebral bodies and pelvic bones, suggestive of metastasis. Subsequently,  $^{18}\text{F}$ -FDG PET/CT done at another institution to detect the primary site of malignancy showed metabolically active cervical, mediastinal, abdominal, pelvic, and inguino-femoral lymphadenopathy. A TruCut (Merit Medical Systems, Inc.) biopsy of the enlarged left cervical lymph node revealed metastatic adenocarcinoma, consistent with a prostatic primary tumor. The prostate-specific

antigen level was elevated (871.87 ng/mL). The patient was treated with leuprolide injection and abiraterone but showed disease progression and was referred to be evaluated for PSMA-targeted radioligand therapy.  $^{68}\text{Ga}$ -PSMA-11 and  $^{18}\text{F}$ -FDG PET/CT whole-body scans were done 60 min after intravenous injection of 122.1 MBq of  $^{68}\text{Ga}$ -PSMA and 111 MBq of  $^{18}\text{F}$ -FDG, using a whole-body full-ring dedicated 3-dimensional PET/CT scanner covering the vertex to the mid-thigh region, as a part of routine workup. It showed  $^{68}\text{Ga}$ -PSMA-11-expressing and  $^{18}\text{F}$ -FDG-avid skeletal lesions and non- $^{68}\text{Ga}$ -PSMA-11-expressing and  $^{18}\text{F}$ -FDG-avid hypodense liver lesions involving segment VII/VIII (Fig. 1). In view of the discordant liver lesions, ultrasonography-guided biopsy of the liver segments was advised and revealed combined hepatocellular carcinoma and cholangiocarcinoma (Fig. 2).  $^{177}\text{Lu}$ -PSMA-617 PSMA-targeted radioligand therapy was considered in view of the  $^{68}\text{Ga}$ -PSMA-11-expressing skeletal lesions, and a posttherapy scan showed  $^{177}\text{Lu}$ -PSMA-617-concentrating skeletal lesions, whereas the hypodense liver lesions did not show any  $^{177}\text{Lu}$ -PSMA-617 uptake (Fig. 3). Subsequently, the patient was managed by a medical oncologist for the combined hepatocellular carcinoma and cholangiocarcinoma.

#### Case 2

A 64-y-old man presented with symptoms of the lower urinary tract for 2 y. On evaluation, ultrasonography of the

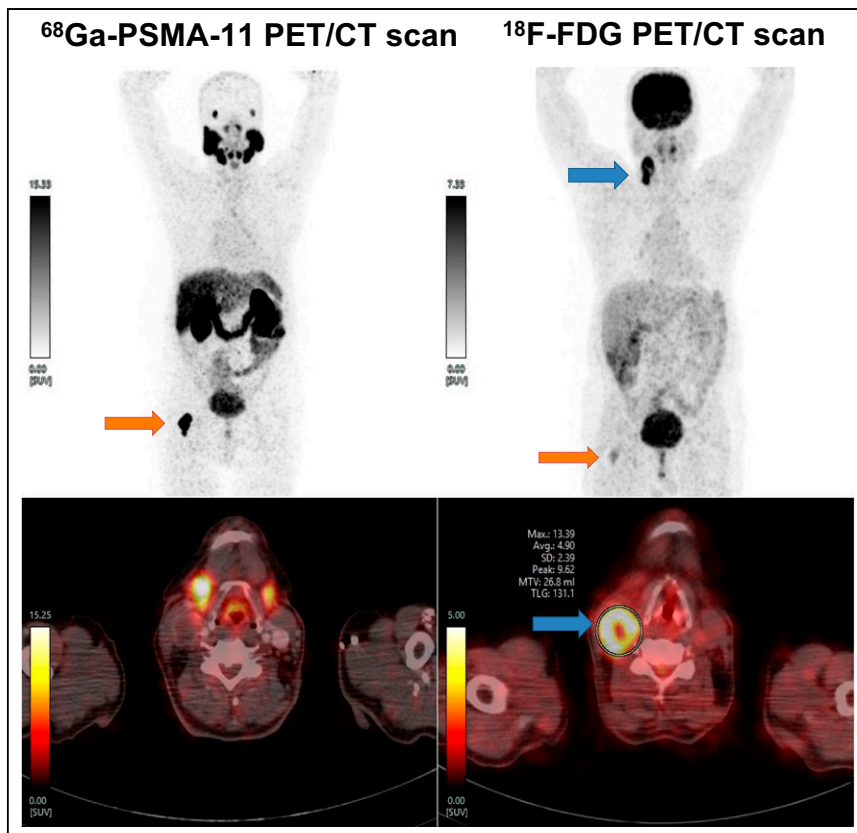


**FIGURE 4.** Whole-body  $^{68}\text{Ga}$ -PSMA-11 PET/CT and  $^{18}\text{F}$ -FDG PET/CT images showing  $^{68}\text{Ga}$ -PSMA-11 expression (orange arrows) in sclerotic lesion involving right neck of femur, and low-grade  $^{18}\text{F}$ -FDG uptake, consistent with diagnosis of prostate carcinoma with skeletal metastasis. Right cervical III/IV lymph node shows  $^{18}\text{F}$ -FDG uptake (blue arrows) but not  $^{68}\text{Ga}$ -PSMA-11 expression, raising suspicion of different pathology.

pelvis revealed the median lobe of the prostate to be enlarged, with increased urinary bladder residue. MRI of the prostate revealed moderate prostatomegaly with a prominent median lobe (Prostate Imaging Reporting and Data System V) and multiple osteolytic lesions in the pelvic bones and bilaterally in the proximal femurs. Spectroscopy showed an increased choline peak and an increased choline-to-citrate ratio. The prostate-specific antigen level was elevated (35.2 ng/mL). Transrectal ultrasound-guided prostate biopsy revealed conventional prostate adenocarcinoma. The patient was treated with degarelix, followed by leuprolide injection and enzalutamide. However, the disease progressed, and the patient was referred to be evaluated for PSMA-targeted radioligand therapy. As a part of the routine work-up, the patient underwent dual-tracer PET/CT. It showed a  $^{68}\text{Ga}$ -PSMA-11-expressing and  $^{18}\text{F}$ -FDG-avid sclerotic skeletal lesion involving the right neck of the femur but non- $^{68}\text{Ga}$ -PSMA-11-expressing and  $^{18}\text{F}$ -FDG-avid right lymphadenopathy at cervical level III/IV (Fig. 4). This discordant lesion raised suspicion; therefore, the patient underwent fine-needle aspiration cytology of the right cervical lymphadenopathy, which turned out to be metastasis of squamous

differentiation. Ultrasonography-guided biopsy of the right cervical lymph node showed poorly differentiated metastatic squamous cell carcinoma.

## DISCUSSION

This report emphasizes the importance of careful evaluation of discordant lesions on dual-tracer PET/CT in metastatic castration-resistant prostate carcinoma patients. The discordant findings on  $^{68}\text{Ga}$ -PSMA-11 and  $^{18}\text{F}$ -FDG PET/CT encountered during routine work up of metastatic castration-resistant prostate carcinoma showed lesions that were  $^{18}\text{F}$ -FDG-avid and non- $^{68}\text{Ga}$ -PSMA-11-avid, raising suspicion. The biopsy of the respective lesions showed SPM of cholangiocarcinoma (first case) and poorly differentiated metastatic squamous cell carcinoma (second case), adding a new dimension to the management in these patients.

A study conducted in Germany by Ulrike Braisch et al. showed that there is a significantly increased risk of several types of SPMs among prostate cancer patients, underscoring the importance of recognizing SPMs. The SPMs were found to be melanoma, leukemia, myeloma, and cancers of the urinary bladder, kidney, pancreas, nervous system, thyroid, and small intestine (11).

The importance of evaluating discordant lesions on dual-tracer PET/CT in the case of neuroendocrine tumors has been reported (12). Incidentally detected primary tumors on  $^{18}\text{F}$ -FDG PET/CT are also not uncommon (13). In our 2 cases, lesions with absence of  $^{68}\text{Ga}$ -PSMA-11 uptake and high uptake on  $^{18}\text{F}$ -FDG PET/CT, which otherwise indicates a different tumor biology commensurate with the aggressiveness of the tumor in carcinoma of the prostate, eventually led to the detection of new SPMs.

## CONCLUSION

This study highlights that appropriate evaluation of discordant lesions on dual-tracer PET/CT ( $^{68}\text{Ga}$ -PSMA-11 and  $^{18}\text{F}$ -FDG PET/CT) can lead to early diagnosis and management of SPMs in patients with prostate carcinoma.

## DISCLOSURE

No potential conflict of interest relevant to this article was reported.

## REFERENCES

1. Jemal A, Center MM, DeSantis C, Ward EM. Global patterns of cancer incidence and mortality rates and trends. *Cancer Epidemiol Biomarkers Prev.* 2010;19:1893–1907.
2. Gann PH. Risk factors for prostate cancer. *Rev Urol.* 2002;4(suppl 5):S3–S10.
3. Wallner LP, Wang R, Jacobsen SJ, Haque R. Androgen deprivation therapy for treatment of localized prostate cancer and risk of second primary malignancies. *Cancer Epidemiol Biomarkers Prev.* 2013;22:313–316.
4. Zelefsky MJ, Housman DM, Pei X, et al. Incidence of secondary cancer development after high-dose intensity-modulated radiotherapy and image-guided brachytherapy for the treatment of localized prostate cancer. *Int J Radiat Oncol Biol Phys.* 2012;83:953–959.
5. Nieder AM, Porter MP, Soloway MS. Radiation therapy for prostate cancer increases subsequent risk of bladder and rectal cancer: a population based cohort study. *J Urol.* 2008;180:2005–2009.
6. Jin T, Song T, Deng S, Wang K. Radiation-induced secondary malignancy in prostate cancer: a systematic review and meta-analysis. *Urol Int.* 2014;93:279–288.
7. Rapiti E, Fioretta G, Verkooijen HM, et al. Increased risk of colon cancer after external radiation therapy for prostate cancer. *Int J Cancer.* 2008;123:1141–1145.
8. Seifert R, Telli T, Hadaschik B, Fendler WP, Kuo PH, Herrmann K. Is  $^{18}\text{F}$ -FDG PET needed to assess  $^{177}\text{Lu}$ -PSMA therapy eligibility? A VISION-like, single-center analysis. *J Nucl Med.* 2023;64:731–737.
9. Ferdinandus J, Violet J, Sandhu S, et al. Prognostic biomarkers in men with metastatic castration-resistant prostate cancer receiving [ $^{177}\text{Lu}$ ]-PSMA-617. *Eur J Nucl Med Mol Imaging.* 2020;47:2322–2327.
10. Buteau JP, Martin AJ, Emmett L, et al. PSMA and FDG-PET as predictive and prognostic biomarkers in patients given [ $^{177}\text{Lu}$ ]-PSMA-617 versus cabazitaxel for metastatic castration-resistant prostate cancer (TheraP): a biomarker analysis from a randomised, open-label, phase 2 trial. *Lancet Oncol.* 2022;23:1389–1397.
11. Braisch U, Meyer M, Radespiel-Tröger M. Risk of subsequent primary cancer among prostate cancer patients in Bavaria, Germany. *Eur J Cancer Prev.* 2012;21:552–559.
12. Kalshetty A, Basu S. Interpreting discordance on dual-tracer positron emission tomography-computed tomography in the setting of metastatic neuroendocrine tumor: detection of metachronous triple-negative breast carcinoma. *World J Nucl Med.* 2020;19:414–416.
13. Kudura K, Ritz N, Templeton AJ, et al. Additional primary tumors detected incidentally on FDG PET/CT at staging in patients with first diagnosis of NSCLC: frequency, impact on patient management and survival. *Cancers (Basel).* 2023;15:1521.